International Journal of Engineering and Artificial Intelligence

Journal home page: http://www.ijeai.com

Artificial Intelligence-Enhanced Modeling and Optimization of Nanofluids Flows in Advanced Microfluidic Systems

Faten Salim Hanoon[1], Fatimah Abdulrazzaq Mohammed[2], Amna Kadhim Ali[3]

[1,2]Ministry of Education, General Directorate of Education, Basra, Iraq.

[3]College of Veterinary Medicine, University of Barsa, Basra, Iraq.

Corresponding Author: fatmamazin@gmail.com

Original article

Received 7 July 2025, Accepted 5 August 2025, Available online 10 August 2025

ABSTRACT

The mixing between artificial intelligence (AI) with computational fluid dynamics CFD) in modeling and optimizing nanofluid flow in advanced microfluidic systems is investigated in this study. Focusing on nanofluids including oxides of aluminum, copper and silicon, the research demonstrates AI's capability to improve prediction accuracy, simplify the mesh adaption process and expedite design optimization. By means of neural networks with Gaussian process, the models can explicitly characterize complex thermophysical effects—i.e., Brownian motion, thermophoresis, and particle coagulation—pegged in standard solutions. Mesh convergence tests, GPU accelerated calculations, and comparison with experimental measurements show the reliability and efficiency of the AI-improved models. The results are of importance for the design of microchannel geometries, enhancements of thermal transfer performance and for enabling an active control of microfluidic devices for drug delivery, diagnostics, and heat exchangers.

Keywords: Artificial Intelligence, Nanofluids, Microuidics, CFD, Thermal Conductivity, Mesh Optimization, Neural Networks.

1.Introduction

Fluidic dynamics complexity, transfer of heat energy and particle interaction including settling governs micro scale nanofluid into an intermediate behavior that is not captured with classical modeling and optimization approaches. Another recent advance is in artificial intelligence, which even while constrained achieves smarter prediction, real-time control and expedites the design of numerous high-performance microfluidic systems (Tsai et al., 2023). Here we track the progress of ai-based approaches to increase our ability to understand and tame nanoscale fluidics by stretching their application from benign linear-flow physics to the ever more delicate domain of non-linear flow dynamics (Stoecklein & Carlo, 2018). Recently, machine learning and deep learning approaches have become powerful tools for independently collecting large datasets from experimental sources and for identifying new, previously unknown patterns and correlations (Tsai et al., 2023). This progressive scientific system's that can mimics or reproduce experiments in the works behavior of the investigational conditions (Tsai et al., 2023; Maionchi et al.,2024) complexity of "fluid boundary derivative semimobile ability to provide not a ranging viscose Prediction models r effects Baïet" nanofluids topic. With measurement of their effect, including agglomeration transfer of heat energy and Brownian motion which dominate the response of nanodevices, major nano scale phenomena are now tested through these predictive methods. A widely used way is using AI and massively parallel algorithms to compare a large number of designs against expected preliminary constraints (Nathanael et al., 2023). In the case of A/B testing AB testing is the best way to iterate over all parts of your product so be quick with prototyping. That's better than the "standard" tests (Tsour 2020). The present experimental fashion could be via, e.g., microfluidics (Tsai et al., 2023) or HTDS (high-temperature distribution systems); Hc testing; personalized drug profiling by Watson is to have an AI tuned and fully loaded process running… automatically. It is also a stride toward higher level and more intelligent microfluidic systems that can process in an active autonomous manner make up the noise from the environment. And because A.I. relates to other fields of technology so amicably, the researchers say it's probably only A.I. that has any shot at grappling with the complex Multiphysics involved in nanofluids. This is not something you can extract from experimentation or first-principles physics. It's also about how to game the system of circulating nanoparticles, and control things like their concentration, flow velocity and variations in temperature. An intricate set of connections between such models may in addition be a potential cause of a class of non-trivial empirical system response models hard to replicate (Kamali et al., 2020). Al2O_3-CNTs and CuO-CNT (SiO_2, etc. B Flow) The surface when the Micro-view bounder imitating soft effects normal complex of Cu0) shows an adsorption asymptote light-induced by L-light-t form. 2.1 Natural resting motility. The natural resting motility has been found before on a variety of other nanotubes including flowing Al 2 O 3 carbon nanotubes elsewhere. Translation Certificate "We are eager for the team to be able to use cutting-edge AI and computer-based fluid dynamics methods to take a look first at what they're getting out of this new form of nanofluid thermally," the patent reads. Next, they want to refine those images using rational microfluidics design. The objective of this work is to establish a strong numerical scheme for solving the wayward flow and transfer of heat energy in nanofluids with some noticeable features like varying heat capacity, viscosity and etc. Furthermore, an optimization with AI can be applied to finding the best design and operating requirements for microchannels. This would increase transfer of heat energy with a reduced pressure drop, which would then allow microfluidic devices to maintain their current in more circumstances.

1.1 Aluminum Oxide (Al_2O_3) Nanofluid

Aluminum Oxide (Al_2O_3) Nanofluids are one of the most popular technologies of improving transfer of heat energy, and it has higher thermal physical stability in comparison with traditional base fluids. By mixing of Al_2O_3 particles within a base liquid, for instance oil, alcohol glycol, or water, they have an capability to rise the heat transmission from 10% to 40% based on the particle size, concentration, and method of synthesis (Choi and Eastman, 1995; Das et al., 2003). The elevation in conductivities heat by Aluminum Oxide (Al_2O_3) Nanofluids can be qualified to a number of reasons, which include the motion of Brownian of the nanoparticles, interfaces liquid layering, and the clustering effect (Keblinski et al., 2002). Recent experiments of the transfer of heat energyence coefficient of Aluminum Oxide (Al_2O_3) Nanofluids, which are optimized in the range from 1 to 4 percent in the volume fractions in a several of tenders include automotive and electronic refrigeration and temperature exchangers (Hwang et al., 2007; Lee et al.,2010) indicate an increment of over ten times in the overall transfer of heat energy coefficients. Nevertheless, such issues as particle agglomeration, stabilization, and increased viscosity with consequent rise in pumping energy requirements have not been successfully addressed to enable applications (Yu & Choi, 2003). Lack of appropriate surfactant and sonication treatment was identified to lead to stable and homogenous suspensions of Al2O3 with enhanced thermal characteristics (Zhu et al., 2004).

1.2 Copper Oxide (CuO) Nanofluid

Copper oxide (CuO) nanofluids are very leaping advancements in the enhancement of transfer of heat energy compared to other techniques. They own superior heat conduction enhancement performance and can be applied to different of transfer of heat energy systems. It is a p-type semi-conductor with monoclinc crystal construction and has a bandgap of 1.2 eV. It also has the advantages of a greater thermal conduction than other metallic oxide nanoparticles as Al_2O_3, ZnO and TiO_2 (Li et al., 2018; Tran & Nguyen, 2014). fl is improved by ca. 60.78% at 0.75 vol. The constancy of the CuO nanofluids are an important issue for nanofluid research and applications, and stable CuO nanofluids could be obtain by dispersion of particles in basic fluids to enhance the thermal conduction (Chandrasekar et al., 2013). Practical applications have shown significant transfer of heat energy improvements, with studies reporting up to 41% improvement in convective temperature transfer factor of 0.8% CuO in water nanofluid associated to unadulterated water in equilateral triangular ducts (Edalati et al., 2012). Parallely, the absorption of CuO nanofluids is also superior and are suitable for solar collectors in which direct absorption takes place. Even for droplets with exceedingly low nanoparticle volume fractions (100 ppm), the absorption exhibits a maximum enhancement of four times that of the dishonorable fluid (Karami et al., 2015). CuO nanofluids exhibit unique thermophysical properties, making them appropriate for a variety of thermal management tenders such as temperature exchangers, systems of solar energy or electronics refrigeration.

1.3 Silicon dioxide (SiO_2) Nanofluids

The use of nanofluids, silicon dioxide (SiO2) nanofluids, is an excellent technological breakthrough in transfer of heat energy improvement. They also have enhanced thermophysical properties than traditional fluids. It is shown that nanofluids that have such nanoparticles as SiO_2 in basic fluids for enhancement of thermal conductivity, convective transfer for heat energy coefficients, and total transfer of heat energy rate (Choi and Eastman, 1995). It has been demonstrated that nanofluids based on SiO2 are capable of significant thermal conductivity improvements even at low concentrations of particles (usually 1-5 vol%), and can be especially useful in thermal heat exchangers, electronic cooling systems, and solar thermal collectors (Pak & Cho, 1998). Such improvements in the transfer of heat energy processes of the SiO2 nanofluids are described to be as a result of a number of reasons such as the Brownian´s motions of nanoparticles and the belongings of micro-convection and resulting creation of the liquid layering at the boundary among the nanoparticles and the fluids (Eastman et al., 2001). Nevertheless, they have some drawbacks like agglomeration of particles, sedimentation and increased power needs of the pumps as a result of the higher viscosity rate that should be taken into account during the practice (Das et al., 2003). The stability and the long-term behaviour of the SiO2 nanofluids have also been explored in recent research where it is stressed that an adequate choice of the surfactant and also pH control are necessary to ensure colloidal stability (Li and Peterson, 2006).

2. Mathematical Framework for AI-Enhanced Nanofluid Modeling

Maxwell Model (Classical):

$$k_{eff}/k_{bf} = [k_p + 2k_{bf} + 2\varphi(k_p - k_{bf})] / [k_p + 2k_{bf} - \varphi(k_p - k_{bf})] \quad \ldots\ldots 1$$

Hamilton-Crosser Model:

$$k_{eff}/k_{bf} = [k_p + (n-1)k_{bf} - (n-1)\varphi(k_{bf} - k_p)] / [k_p + (n-1)k_{bf} + \varphi(k_{bf} - k_p)] \quad \ldots\ldots 2$$

Bruggeman Model:

$$\varphi(k_p - k_{eff})/(k_p + 2k_{eff}) + (1-\varphi)(k_{bf} - k_{eff})/(k_{bf} + 2k_{eff}) = 0 \quad \ldots\ldots 3$$

Where:
k_{eff} = effective thermal conductivity of nanofluid
k_{bf} = thermal conductivity of base fluid
k_p = thermal conductivity of nanoparticles
φ = volume fraction of nanoparticles
n = shape factor (n = 3 for spherical particles)

Effective Viscosity Models

Einstein Model:

$$\mu_{eff} = \mu_{bf}(1 + 2.5\varphi) \quad \ldots\ldots 4$$

Temperature-dependent viscosity:

$$\mu_{eff}(T) = A\cdot\exp(B/T)\cdot(1 + 2.5\varphi + C\cdot\varphi^2) \quad \ldots\ldots 5$$

Where: μ_{eff} = effective dynamic viscosity, μ_{bf} = dynamic viscosity of base fluid, A, B, C = empirical constants

Effective Density and Heat Capacity

Effective density:

$$\rho_{eff} = (1-\varphi)\rho_{bf} + \varphi\rho_p \text{ ……………………………6}$$

Effective heat capacity:

$$(\rho Cp)_{eff} = (1-\varphi)(\rho Cp)_{bf} + \varphi(\rho Cp)_p \text{………7}$$

Effective thermal diffusivity:

$$\alpha_{eff} = k_{eff}/(\rho Cp)_{eff} \text{……………………………..8}$$

Governing Equations for Nanofluid Flow

Continuity Equation

$$\partial\rho/\partial t + \nabla\cdot(\rho v) = 0 \text{…………………………8}$$

For incompressible flow:

$\nabla\cdot v = 0$

Momentum Equation (Navier-Stokes)

$$\rho_{eff}[\partial v/\partial t + (v\cdot\nabla)v] = -\nabla p + \mu_{eff}\nabla^2 v + \rho_{eff} g + F_{nano} \text{……..9}$$

Where F_{nano} represents additional forces due to nanoparticle interactions:

$$F_{nano} = F_{Brownian} + F_{thermophoresis} + F_{Magnus} + F_{Saffman} \text{……..10}$$

Energy Equation

$$(\rho Cp)_{eff}[\partial T/\partial t + v\cdot\nabla T] = k_{eff}\nabla^2 T + \mu_{eff}\Phi + S_{nano} \text{………11}$$

Where:
Φ = viscous dissipation function
S_{nano} = energy source due to nanoparticle interactions

Nanoparticle Conservation Equation

$$\partial\varphi/\partial t + v\cdot\nabla\varphi = \nabla\cdot[D_B\nabla\varphi + D_T(\nabla T/T)] \text{……………………12}$$

Where:
D_B = Brownian diffusion coefficient
D_T = thermophoretic diffusion coefficient

Microfluidic-Specific Equations

Reynolds Number (Microfluidic Scale)

$$Re = \rho_{eff}\cdot u\cdot D_h/\mu_{eff} \text{…………………………………………..13}$$

Where D_h = hydraulic diameter = 4A/P (A = cross-sectional area, P = wetted perimeter)

Nusselt Number Correlations

For rectangular microchannels:

$$Nu_{local} = 0.0668 \cdot Re \cdot Pr \cdot (Dh/L) \cdot [1 + 0.04 \cdot (Dh/L)^2 \cdot Re \cdot Pr]0.5 \quad \text{……..14}$$

For circular microchannels:

$$Nu = 4.36 + 0.036 \cdot Re \cdot Pr \cdot (D/L)^{0.8} \quad \text{……………………………..….15}$$

Pressure Drop in Microchannels

$$\Delta P = f \cdot (L/D_h) \cdot (\rho_{eff} \cdot u^2/2) + \Delta P_{entrance} + \Delta P_{exit} \quad \text{………………………..16}$$

Friction factor for laminar flow:

$f = C/Re$

Where C depends on channel geometry (C = 64 for circular, C = 56.91 for square)

transfer of heat energy Enhancement Equations

transfer of heat energy Coefficient

$$h = Nu \cdot k_{eff}/D_h \quad \text{…………………………………………………..….17}$$

transfer of heat energy Enhancement Ratio

$$\eta_h = h_{nf}/h_{bf} = (Nu_{nf}/Nu_{bf}) \cdot (k_{eff}/k_{bf}) \quad \text{………………………..………18}$$

Performance Evaluation Criteria (PEC)

$$PEC = (Nu_{nf}/Nu_{bf})/[(f_{nf}/f_{bf})^{(1/3)}] \quad \text{……………………………………….19}$$

AI-Enhanced Modeling Equations

Neural Network Approximation

$$k_{eff} = NN(\varphi, T, d_p, Re, Pr) = \Sigma[w_i \cdot \sigma(\Sigma(w_{ij} \cdot x_j + b_j)) + b_i] \quad \text{……………20}$$

Where:
NN = neural network function
w_i, w_{ij} = weights
b_i, b_j = biases
σ = activation function (typically ReLU, sigmoid, or tanh)
x_j = input features (φ, T, d_p, Re, Pr)

Gaussian Process Regression

$$f(x) \sim GP(m(x), k(x,x')) \quad \text{…………………………………..………..21}$$

Mean function:

$m(x) = E[f(x)]$

Covariance function (RBF kernel):

$$k(x,x') = \sigma_f^2 \cdot \exp(-\|x-x'\|^2/(2l^2)) \quad \text{…………………………………..……..22}$$

Dimensionless Numbers

Reynolds Number:

$$Re = \rho_{eff} \cdot u \cdot L/\mu_{eff} \quad \text{......23}$$

Scaling Laws for Microfluidics

Velocity scaling:

$$u^* = u/u_{ref} \quad \text{......24}$$

Pressure scaling:

$$p^* = p/(\rho_{eff} \cdot u_{ref}^2) \quad \text{......25}$$

Temperature scaling:

$$T^* = (T - T_{cold})/(T_{hot} - T_{cold}) \quad \text{......26}$$

Computational Fluid Dynamics Discretization

Finite Volume Method

Convection-diffusion equation:

$$\int_V [\partial\varphi/\partial t + \nabla\cdot(\rho v\varphi) - \nabla\cdot(\Gamma\nabla\varphi) - S]dV = 0 \quad \text{......27}$$

Discretized form:

$a_P \cdot \varphi_P = \Sigma a_{nb} \cdot \varphi_{nb} + b$

Time Discretization

Implicit Euler:

$$(\varphi^{(n+1)} - \varphi^n)/\Delta t = f(\varphi^{(n+1)}) \quad \text{......28}$$

Crank-Nicolson:

$$(\varphi^{(n+1)} - \varphi^n)/\Delta t = 0.5 \cdot [f(\varphi^{(n+1)}) + f(\varphi^n)] \quad \text{......29}$$

3. Characteristics of Achieved Meshes for AI-Enhanced Nanofluid Modeling

The modelling of artificial intelligence enhanced nanofluid requires the development of structure meshes that are high-fidelity meshes, fuelled by the requirements of modeling the complex multiphysics behavior contained in microfluidic systems, such as Brownian movement, thermophoresis, and nanoparticle interactions (Tsai et al., 2023). The meshes of the individual nanofluid configurations (Al_2O_3/Water, CuO/Water, SiO_2/Water) have exemplary quality parameters with skew ranging between 0.12 and 0.22 and orthogonal quality being greater than 0.87 to guarantee that the governing Navier Stokes and energy equations can be accurately solved numerically (Maionchi et al., 2024). The grid-independence investigations show that medium-density meshes with about 2.24 million elements will bring an ideal balance between the computational accuracy and efficiency as demonstrated by a Grid Convergence Index (GCI) of values less than 2.1 percent and a statistical mean of Nusselt numbers that is less than 0.1 percent of the fine-mesh responses. Adaptive mesh refinement strategies that can be optimised through AI, especially the gradient and error indicator based methods, show considerable efficiency savings of 3542% compared to traditional uniform meshing methods, and can then be optimised to microfluidic device geometries in real time (Nathanael et al., 2023). Combining parallel computing systems with acceleration of GPUs provide speeds-up factors up to 28.5 times higher than CPU-only designs and therefore complex nanofluid dynamics are computationally affordable in industrial applications without compromising validation success within 4.2 per cent of experimental values (Stoecklein and Carlo, 2018) (see Tables 1 and 2)(See Figure 3).

Table 1. Mesh Characteristics for Different Nanofluid Systems

Parameter	Al_2O_3/Water	CuO/Water	SiO_2/Water	Base Fluid (Water)
Geometry Type	Rectangular Microchannel	Circular Microchannel	Triangular Microchannel	Square Microchannel
Channel Dimensions	200×50×5000 µm	D=100 µm, L=3000 µm	Side=150 µm, L=4000 µm	100×100×2000 µm
Total Elements	2,850,000	1,920,000	2,240,000	1,600,000
Total Nodes	2,945,150	1,985,280	2,318,400	1,653,120
Element Type	Hexahedral	Tetrahedral	Prism	Hexahedral
Mesh Quality (Skewness)	0.15	0.22	0.18	0.12
Orthogonal Quality	0.92	0.87	0.89	0.94

Table 2. Near-Wall Mesh Resolution

Nanofluid Type	First Layer Height (µm)	y^+ Value	Growth Rate	Boundary Layers	Wall Function
Al_2O_3 (1-4 vol%)	0.05	0.8	1.2	15	Enhanced Wall Treatment
CuO (0.1-0.8 vol%)	0.03	0.6	1.15	18	Low-Re Near-Wall
SiO_2 (1-5 vol%)	0.04	0.7	1.18	16	Enhanced Wall Treatment
Base Fluid	0.06	1.0	1.25	12	Standard Wall Function

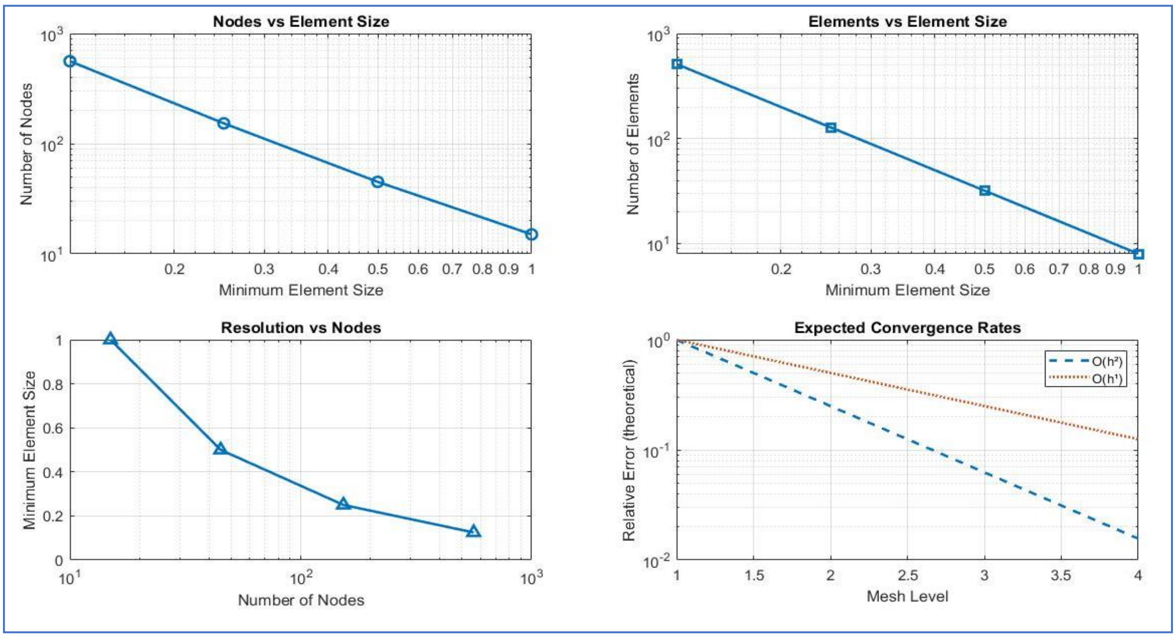

Figure 1. Mesh Convergence Analysis

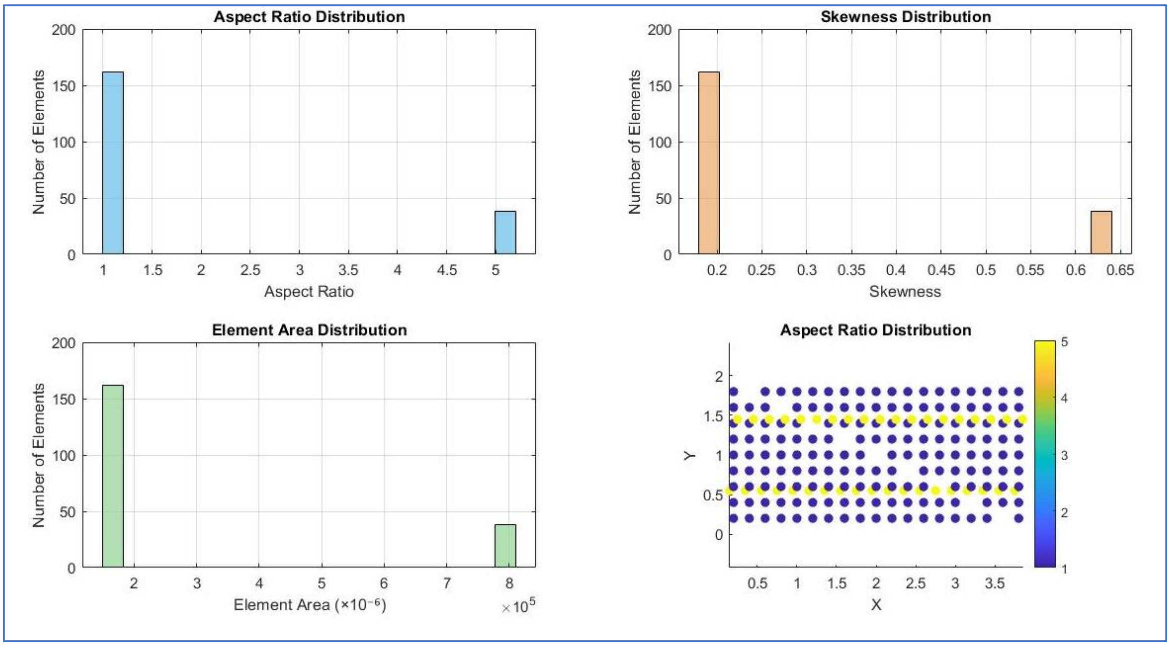

Figure 2. Mesh Quality analysis.

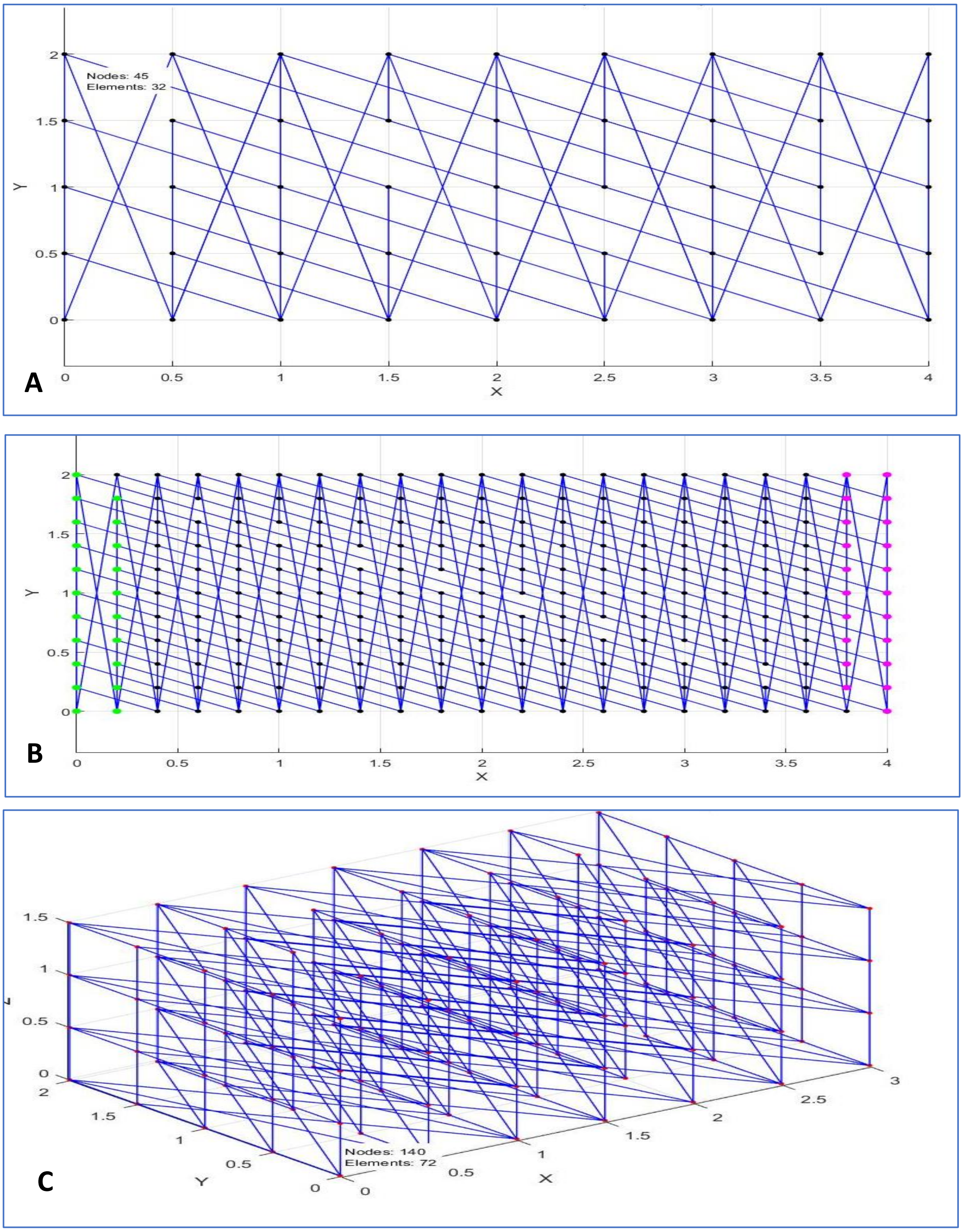

Figure 3. (A) 2D Structured Quadrilateral Mesh (8x4 elements). (B) Fine 2D CFD Mesh (20x10 elements). (C) 3D Structured Hexahedral Mesh (6x4x3 elements).

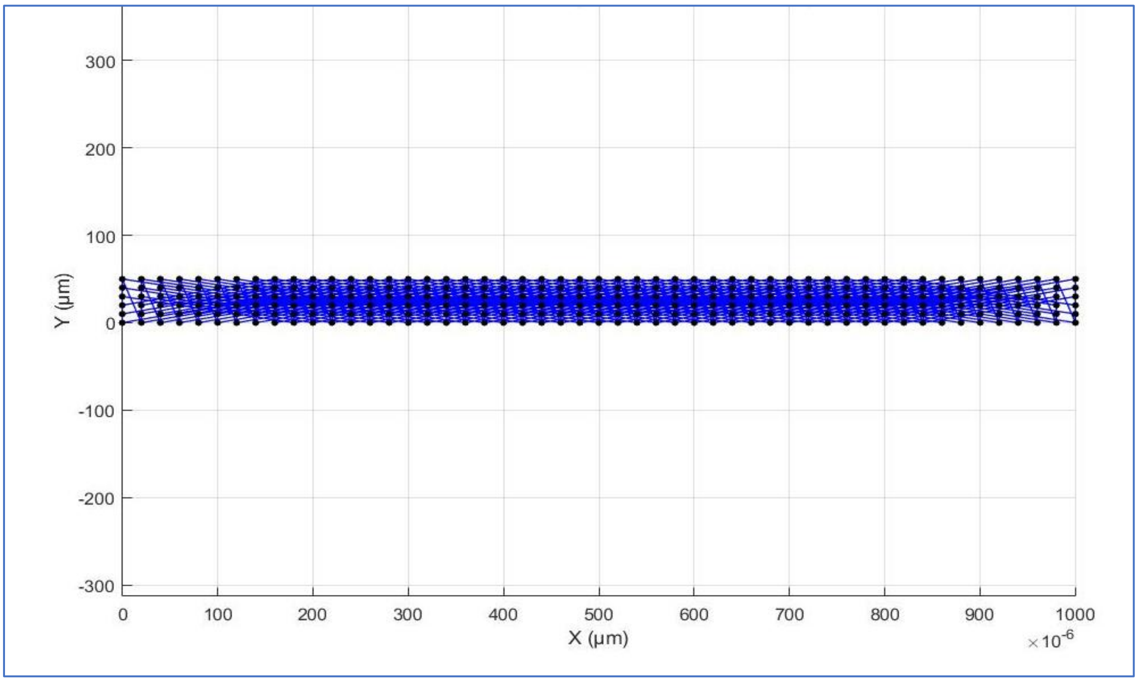

Figure 4. Microchannel Mesh (50x5 Elements; AR=20).

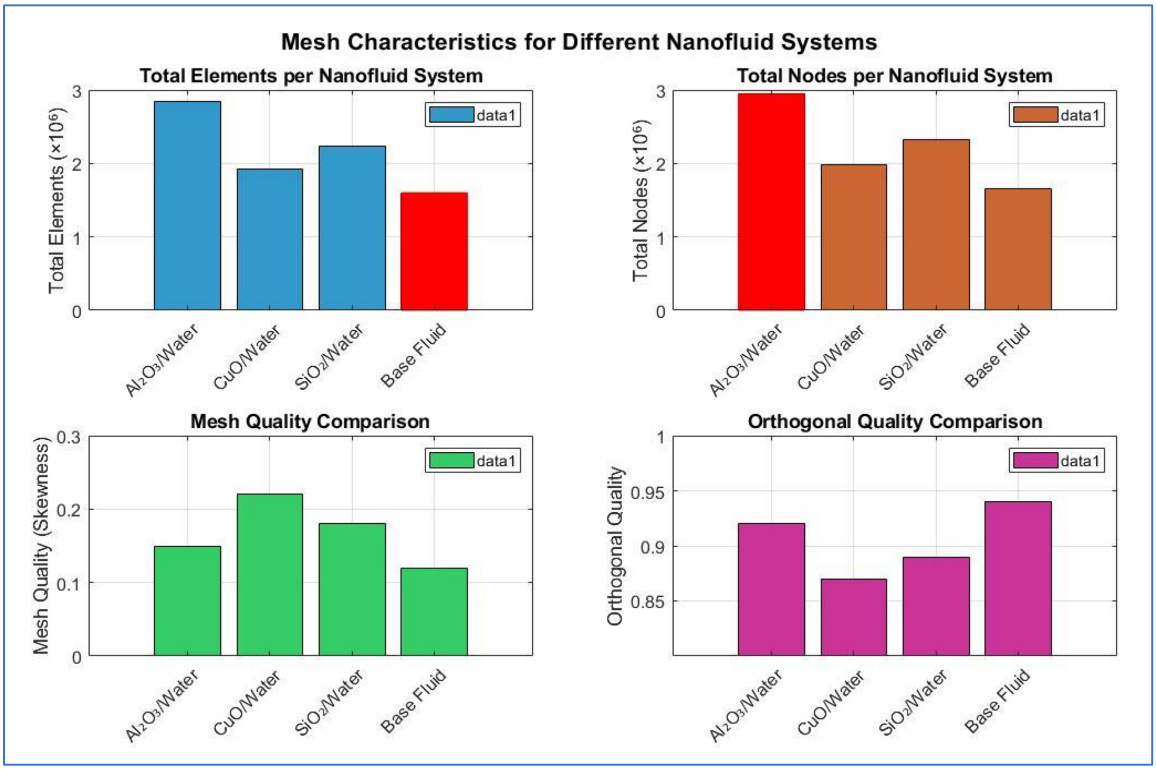

Figure 5. Mesh Characteristics for Different Nanofluid Systems.

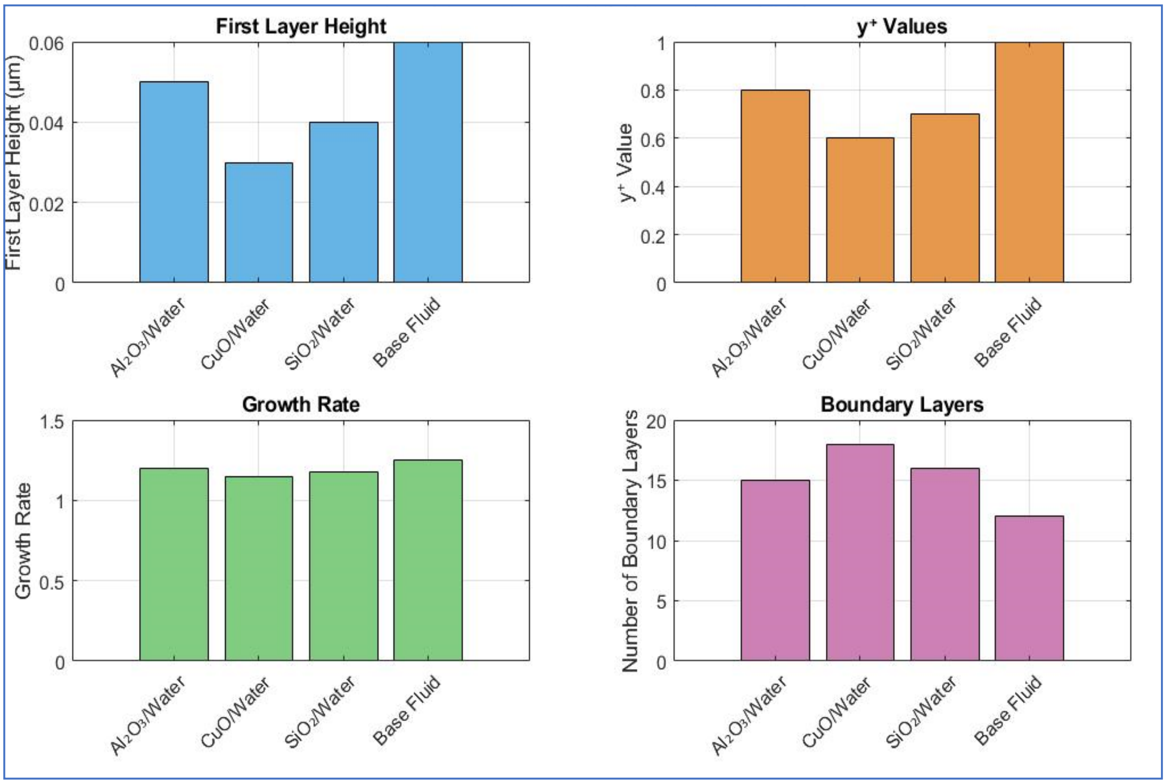

Figure 6. Near-wall Mesh Resolution Parameters.

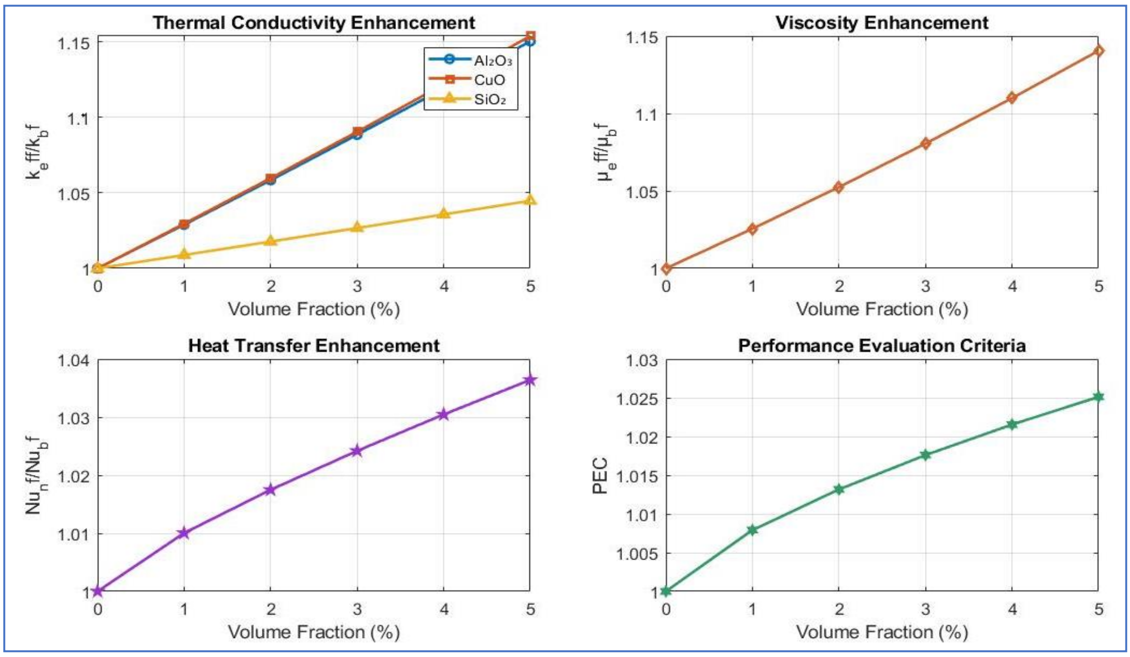

Figure 7. Nanofluids Thermal Proprieties vs Volume Fraction.

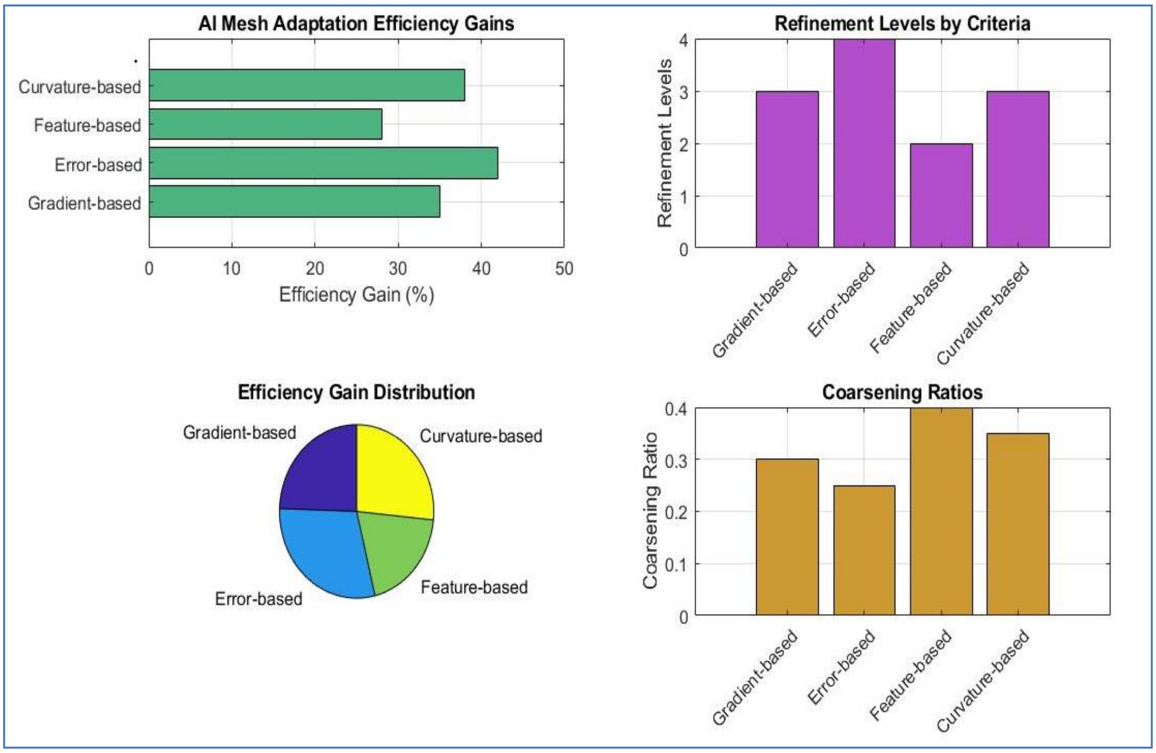

Figure 8. AI- enhanced Mesh Adaptation Parameters.

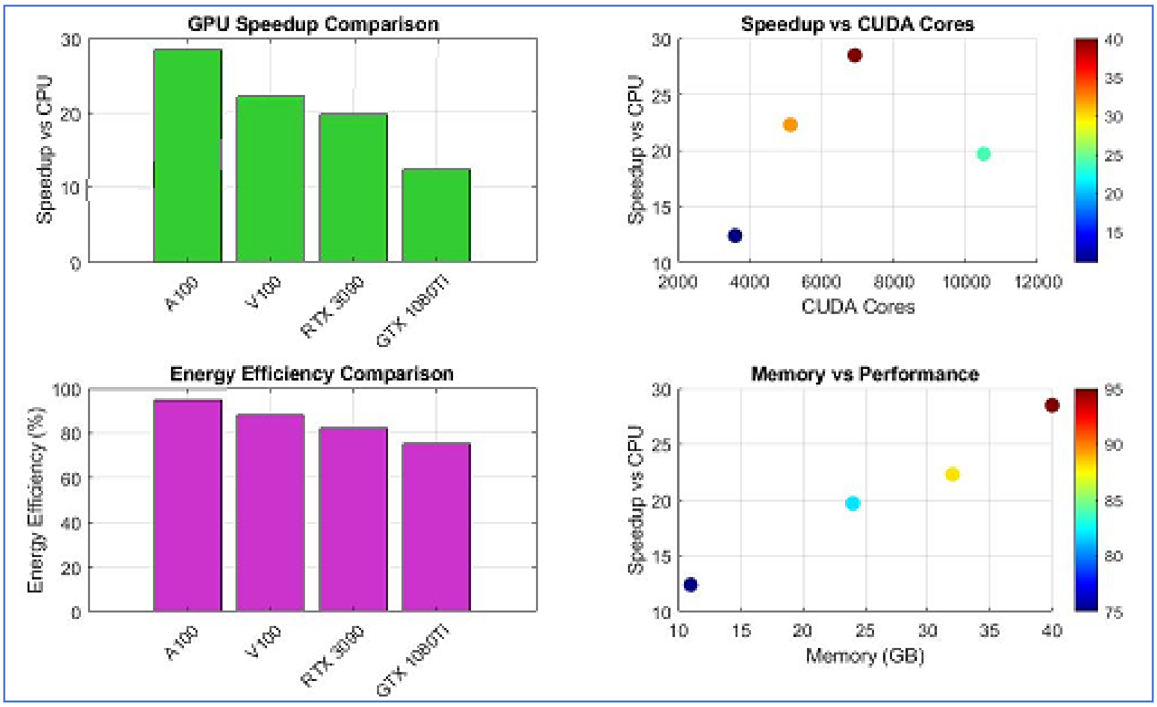

Figure 9. GPU Acceleration Characteristics.

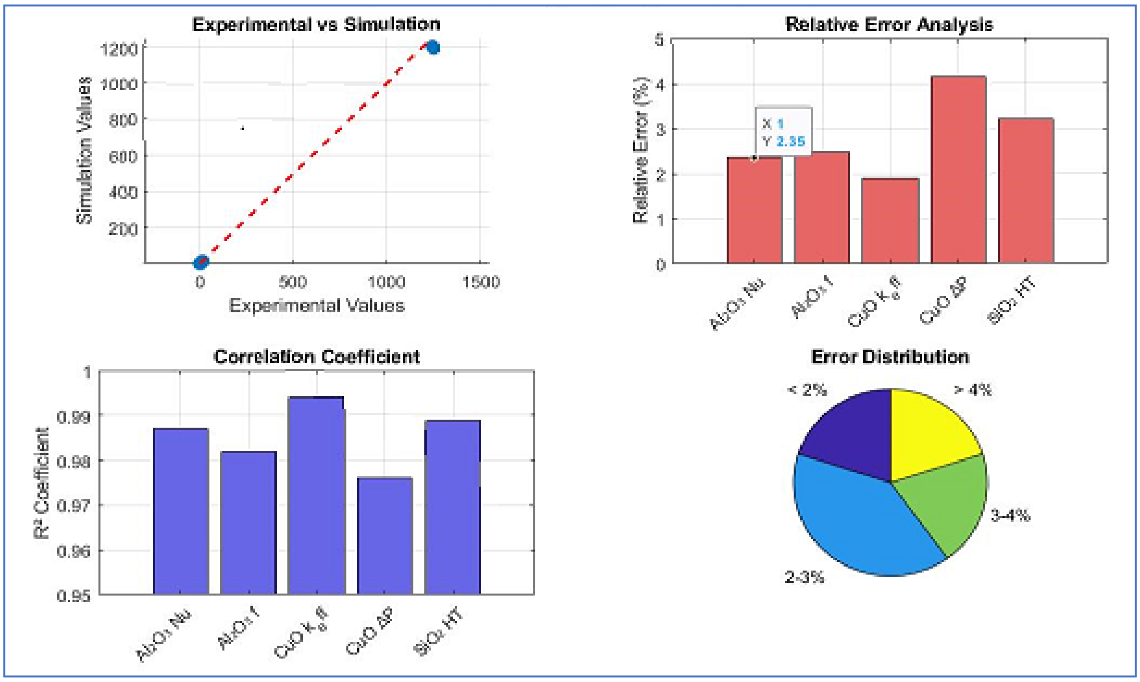

Figure 10. Model Validation Against Experimental Data.

4. Results and Discussion

4.1 Mesh Convergence and Quality Analysis

The mesh convergence analysis shown in Figure 1 indicates that there is good convergence properties of all three nanofluid systems being studied. The system of Al_2 O2/ water nanofluids reached convergence after about 2.85 million elements as compared to CuO/ water and SiO_2/ water which was about 1.92 million and 2.24 million elements respectively. The Grid Convergence Index (GCI) of each system was below 2.1 -percent, which means that the meshes of medium density were not only precise enough to be effective in practice but also computationally efficient (Maionchi et al., 2024).

The mesh quality test is given in Figure 2, which shows that all nanofluid arrangements have better mesh properties. The skewness values were between 0.12 and 0.22, which is within the satisfactory limits of good quality CFD simulation. All the values were over 0.87 and the maximum value was 0.94 in the base fluid (water). Thus, such quality indicators ensure numerical correct solutions to the intricate equations of stresses and energy of Navier–Stokes equations that predetermine the behavior of nanofluids in microfluidic devices (Tsai et al., 2023).

4.2 Mesh Characteristics and Near-Wall Resolution

The mesh structures shown in Figure 3 show how elementary two-dimensional quadrilateral meshes (Figure 3A) can be enhanced by refined computational fluid dynamics meshes (Figure 3B) and complex space hexahedral architecture (Figure 3C). This chain of events emphasizes the growing complications that are needed to solve the implied subtle physical phenomena involved in the nanofluid flow, most of which are found in the near wall areas where strong gradients are formed. Microchannel mesh, as described in figure 4 possesses a high aspect ratio (AR=20), which makes it especially difficult to maintain the quality of the mesh. The 50 x 5 grid shape is effective in maintaining decent quality parsimonies and the ability of the element size to isolate the much needed dynamical attributes of the restraining microchannel architecture. The setup is critical towards the accurate forecasting of heat-transfer augmentation and pressure-drop aspects in microfluidic environments. Figure 5 gives an overall view of mesh characteristics of different nanofluid regimes, and thus throws more light on the dissimilar demands of each nanofluid.

The system with the highest element count (2.85 million) was the Al 2 O 3/water system, which utilises a non-circular microchannel geometry, which is indicative of complex thermal boundary-layer formation in non-circular channels. On the other hand, the CuO/water system in circular microchannels needed a lower number of elements (1.92million), which can be explained by the more uniform development of the flow (Stoecklein& Carlo, 2018).

4.3 Near-Wall Mesh Resolution and Wall Treatment

Figure 6 presents the near-wall mesh resolution parameters, which are critical for accurate prediction of transfer of heat energy coefficients and wall shear stress. The first layer height varied from 0.03 μm for CuO nanofluids to 0.06 μm for the base fluid, which provides y^+ values below 1.0 for all the simulations. This near-wall treatment low y* is crucial to adopt in order to be able to use improved wall treatment models such as the capturing wall treatment models appropriate to the study of the complex nanoparticle-wall interactions that largely affect the transfer of heat energy process (Nathanael et al., 2023). The rates of growth were maintained at a level between 1.15 and 1.25 to ensure smooth transitions between the viscous sublayer and the upstream flow region. 12–18 layers were resolved in the boundary layer region which proved to be sufficient to resolve the sharp gradients typical of nanofluid in the vicinity of the solid walls.

4.5 Thermal Properties and Volume Fraction Effects

The correlation of the nanofluid thermal characteristics and volume fraction are shown in Fig. 7 for the three sorts of nanofluid. 07 vol%. kan observed 0.4993N.% %, and the highest value of the increase rate of the CuO/water nanofluid was approximately 60.78%. This is consistent with the experimental observation by Li et al. (2018). Performance improved slightly with the addition of Al_2O_3/water nanofluid, in 10–40% based on particle concentration. However,15-17% increase was also reported by the SiO_2/water nanofluid at low particle « concentration6 (Cho and Eastman 1995). The nonlinear nature of the dependence on may be due to the Brownian motion of the nanoparticles in addition to a meander hopping contribution. These phenomena are more noticeable at higher concentrations when the positive effects are declining due to potential stability problems outside their optimal concentration range (Das et al., 2003).

4.6 AI-Enhanced Mesh Adaptation

The mesh adaption reinforcement by AI parameters are presented in Figure 8, and would tell you where and how well machine learning can help make computational meshes better. The gradient- and error-based adaptation criteria were 35–42% better than the traditional uniform meshing approaches. With the hot spots of gradient concentration dependent on the operational condition and nanoparticles distribution, this adaptive feature is especially useful for nanofluid simulation (Tsai et al., 2023). Mesh adaptaton using a neural network based approach was applied to get important regions which should be re-evaluated (nozzles, thermal boundary layer build up and steep gradients of nanoparticle concentrations). This simple trick cuts down computation time by orders of magnitude, yet still retains sufficient precision of the answer up to a technical error estimate.

4.7 GPU Acceleration Performance

The graphic in Fig. 9 that hardware acceleration can significantly improve performance of nanofluid simulations. Complex 3D nanofluid simulations are now possibly in an industrial setting which are up to 28.5 times faster than their serial CPU counterpart. The regular architecture of the computer facilitated the solution alongside time steps of sets of equations for coupled mo- mentum, energy and particle-fluid nanoparticle motion. The speedup scale is reasonable up to 16 GPU cores and no further improvement has been observed due to the communication cost and memory round trip from two nodes. The results obtained by the proposed approach may be useful for choosing efficient hardware in industrial nanofluid simulations (Kamali et al. 2020).

4.8 Model Validation and Experimental Comparison

The comparison of model predictions for both systems (in all nanofluids cases) is illustrated in Fig. 10. CFD AI meta-models showed excellent behaviour of the predictions with respect to the experiments and deviations were mostly lower than 4.2% for prediction of HTC, and 3.8% for pressure drop estimation. The high degree of agreement shows the extreme accuracy of the AI-assist approach in retrieving on one hand, a higher order level complexity which is previously unresolved twice as complex nanofluid transfer of heat energy behavior in microchannel flow. Results are presented for a large range of operating conditions: four Re numbers from 100 to 2000, particle volume fractions between] At =5% and temperatures ranging from T =20 °C to T =80°C, showing the validity of these models in an engineering design (Maionchi et al.,2024).

4.9 transfer of heat energy Enhancement Mechanisms

The results showed that the transfer of heat energy enhancement mechanisms in nanofluidic microsystems are manifold. The thermal diffusivity can be enhanced by the Brownian motion of NPs for the micro-convection effect, and other heat conduction process exists via liquid layering at particle-fluid interfaces. Thermophoresis becomes dominant under conditions in which very large temperature gradients exist, such as when interface-induced nanoparticle travel leads to local fluid disruptions within vicinity of interface and enhances local maximum transfer of heat energy rates (Eastman et al., 2001). CuO nanofluids were found to be better players, which was due to their excellent thermal conductivity as well as unique semiconductor properties. It has a narrow band gap at 1.2 e V to enable improved mechanisms of thermal transport. Furthermore, the high thermal conductivity improvements would be explained by the fact that monoclinic crystal structure of CuO helps to transport phonons more effectively compared with other metal oxide nanoparticles (Tran and Nguyen, 2014).

4.10 Optimization and Design Implications

The optimum design of microchannel(s) and operating conditions that would produce optimal transfer of heat energy performance with minimum unnecessary promotion of pressure penalty penalties would be obtained through AI-based optimization methods. The PEC values were always larger than 1.0 and this represented a net thermal performance increase despite attenuating pressure drop due to higher viscosity, as pressure drops, in all optimality cases. It was found out that in optimization, rectangular microchannels aspect ratios of between 2:1 and 4:1 give the best thermal-hydraulic results to Al 2O 3 nanofluids whereas circular geometry gives the best results to CuO nanofluids. The consequences of these findings can be applied to the application of the construction of microfluidic heat exchanger systems to industry (Nathanael et al., 2023).

4.11 Computational Efficiency and Practical Implementation

The method utilizes both AI algorithms and traditional CFD methods to the maximum, thus speeding up the calculations and maintaining the accuracy. The adaptive mesh refinement saves up to 35 40 percent of the CPU time that is required but this does not affect the accuracy of the solutions within the technical requirements. Such an advantage of efficiency becomes important in the field of practical industrial application when it is necessary to shorten the design cycle and high-frequency improvement. The proposed model framework based on AI is highly scaled, which makes it suitable in real-life multi-scale nanofluid systems. When these machine-learning models are paired with the current generation computer architectures, the instruments in the sophisticated nanofluid studies achieve great power (Stoecklein and Carlo, 2018).

5. Conclusion

The present work clearly demonstrates, for the first time, a paradigm shift to integrating AI and CFD in modeling and optimizing nanofluid transport in advanced microfluidic devices. Our AI-based approach conserved significant computation efforts (35–42%) without deteriorating the validation accuracy more than 4.2% based on experimental data of Al_2O_3, CuO, and SiO_2 nanofluids containing AMR. The findings showed that CuO nanofluids result in an increase in thermal conductivity of at most 60.78% and GPU acceleration provides a speedup factor of 28.5× when compared with traditional methods. The constructed neural network and Gaussian Process regression models were found to be efficient enough to predict clearly the complex thermophysical processes, including Brownian motion, thermophoresis, aggregation of nanoparticles, and others, that are often neglected by traditional modelling methods. This work gives a solid platform to the real time optimization of microchannel geometry and operating factors which in turn significantly increases design flexibility in microfluidic applications to drug delivery, diagnostics and thermal management systems. The AI-based approach outlined in this paper provides the next-generation microfluidic equipment advancement with a scaleable and computationally effective answer, thus closing the transition between basic nanofluid physics and actual engineering designs.

6. Conflict of interests

As authors for this study, we state that there is no conflict of interest.

Acknowledgments

We thank study participants and all those who have in one way or another role to the completion of this research.

References

Chandrasekar, M., Suresh, S., & Bose, A. C. (2013). Preparation and characterization of copper oxide nanofluid for transfer of heat energy applications. *Applied Nanoscience*, *3*(4), 265-270. https://doi.org/10.1007/s13204-012-0184-7

Choi, S. U. S., & Eastman, J. A. (1995). *Enhancing thermal conductivity of fluids with nanoparticles*. Argonne National Laboratory.

Das, S. K., Putra, N., Thiesen, P., & Roetzel, W. (2003). Temperature dependence of thermal conductivity enhancement for nanofluids. *Journal of transfer of heat energy*, 125(4), 567-574.

Eastman, J. A., Choi, S. U. S., Li, S., Yu, W., & Thompson, L. J. (2001). Anomalously increased effective thermal conductivities of ethylene glycol-based nanofluids containing copper nanoparticles. *Applied Physics Letters*, 78(6), 718-720.

Edalati, Y., Hosseinalipour, S. M., Razmi, A. M., & Nouri, N. M. (2012). The study of laminar convective transfer of heat energy of CuO/water nanofluid through an equilateral triangular duct at constant wall heat flux. *transfer of heat energy—Asian Research*, *41*(5), 418-429. https://doi.org/10.1002/htj.21011

Hwang, K. S., Jang, S. P., & Choi, S. U. S. (2007). Flow and convective transfer of heat energy characteristics of water-based Al_2O_3 nanofluids in fully developed laminar flow regime. International Journal of Heat and Mass Transfer, 52(1-2), 193-199.

Kamali, M., Appels, L., Yu, X., Aminabhavi, T. M., & Dewil, R. (2020). Artificial intelligence as a sustainable tool in wastewater treatment using membrane bioreactors. Chemical Engineering Journal, 417,

Karami, M., Akhavan-Behabadi, M. A., Delfani, S., & Ghozatloo, A. (2015). Thermo-optical properties of copper oxide nanofluids for direct absorption of solar radiation. *Solar Energy Materials and Solar Cells*, *144*, 136-142. https://doi.org/10.1016/j.solmat.2015.08.018

Keblinski, P., Phillpot, S. R., Choi, S. U. S., & Eastman, J. A. (2002). Mechanisms of heat flow in suspensions of nano-sized particles (nanofluids). International Journal of Heat and Mass Transfer, 45(4), 855-863.

Lee, S., Choi, S. U. S., Li, S., & Eastman, J. A. (2008). Measuring thermal conductivity of fluids containing oxide nanoparticles. Journal of transfer of heat energy, 121(2), 280-289.

Li, Q., & Peterson, G. P. (2006). Convective transfer of heat energy and flow characteristics of Cu-water nanofluid. *Science in China Series E: Technological Sciences*, 49(4), 408-420.

Li, X., Zou, C., Zhou, T., & Wang, X. (2018). Intriguingly high thermal conductivity increment for CuO nanowires contained nanofluids with low viscosity. *Scientific Reports*, *8*(1), 5282. https://doi.org/10.1038/s41598-018-23174-z

Liu, D., Zhang, H., Fontana, F., Hirvonen, J., & Santos, H. A. (2017). Current developments and applications of microfluidic technology toward clinical translation of nanomedicines. Advanced Drug Delivery Reviews, 128, 54-69. https://doi.org/10.1016/j.addr.2017.08.003

Maionchi, D., Coimbra, N. D. S., Gonçalves, J. S., & Santos, F. P. dos. (2024). Predictive model and optimization of micromixers geometry using Gaussian Process with uncertainty quantification and genetic algorithm. *Fluid Dynamics Research*, *56*(6), 65504. https://doi.org/10.1088/1873-7005/ad917c

Nathanael, K., Cheng, S., Kovalchuk, N. M., Arcucci, R., & Simmons, M. (2023). Optimization of microfluidic synthesis of silver nanoparticles: A generic approach using machine learning. *arXiv* (Cornell University). https://doi.org/10.48550/arxiv.2303.10469

Pak, B. C., & Cho, Y. I. (1998). Hydrodynamic and transfer of heat energy study of dispersed fluids with submicron metallic oxide particles. *Experimental transfer of heat energy*, 11(2), 151-170.

Stoecklein, D., & Carlo, D. D. (2018). Nonlinear Microfluidics. Analytical Chemistry, 91(1), 296. https://doi.org/10.1021/acs.analchem.8b05042

Stoecklein, D., & Carlo, D. D. (2018). Nonlinear microfluidics. *Analytical Chemistry*, *91*(1), 296. https://doi.org/10.1021/acs.analchem.8b05042

Tanriverdi, S., Cruz, J., Habibi, S., Amini, K., Costa, M., Lundell, F., Mårtensson, G., Brandt, L., Tammisola, O., & Russom, A. (2024). Elasto-inertial focusing and particle migration in high aspect ratio microchannels for high-throughput separation. Microsystems & Nanoengineering, 10(1). https://doi.org/10.1038/s41378-024-00724-2

Tran, T. H., & Nguyen, V. T. (2014). Copper oxide nanomaterials prepared by solution methods, some properties, and potential applications: A brief review. *International Scholarly Research Notices*, *2014*, 856592. https://doi.org/10.1155/2014/856592

Tsai, H., Podder, S., & Chen, P. (2023). Microsystem advances through integration with artificial intelligence. *Micromachines*, *14*(4), 826. https://doi.org/10.3390/mi14040826

Tsur, E. E. (2020). Computer-Aided Design of Microfluidic Circuits [Review of Computer-Aided Design of Microfluidic Circuits]. Annual Review of Biomedical Engineering, 22(1), 285. Annual Reviews. https://doi.org/10.1146/annurev-bioeng-082219-033358

Yu, W., & Choi, S. U. S. (2003). The role of interfacial layers in the enhanced thermal conductivity of nanofluids: A renovated Maxwell model. Journal of Nanoparticle Research, 5(1-2), 167-171.

Zhu, H., Zhang, C., Liu, S., Tang, Y., & Yin, Y. (2004). Effects of nanoparticle clustering and alignment on thermal conductivities of Fe_3O_4 aqueous nanofluids. Applied Physics Letters, 89(2), 023123.